Cell Proliferation

*Cell Prolif.*, 2015, **48**, 517–531 doi: 10.1111/cpr.12205

# Adult neural progenitor cells from Huntington's disease mouse brain exhibit increased proliferation and migration due to enhanced calcium and ROS signals

Wenjuan Xie*, Jiu-Qiang Wang*, Qiao-Chu Wang*, Yun Wang*, Sheng Yao† and Tie-Shan Tang*

**State Key Laboratory of Biomembrane and Membrane Biotechnology, Institute of Zoology, Chinese Academy of Sciences, Beijing 100101, China and †Department of Neurology, Navy General Hospital, Beijing 100048, China*

*Received 9 March 2015; revision accepted 10 June 2015*

## Abstract

*Objectives*: Huntington's disease (HD) is an inherited human neurodegenerative disorder characterized by uncontrollable movement, psychiatric disturbance and cognitive decline. Impaired proliferative/differentiational potentials of adult neural progenitor cells (ANPCs) have been thought to be a pathogenic mechanism involved in it. In this study, we aimed to elucidate intrinsic properties of ANPCs subjected to neurodegenerative condition in YAC128 HD mice.

*Materials and methods*: ANPCs were isolated from the SVZ regions of 4-month-old WT and YAC128 mice. Cell proliferation, migration and neuronal differentiation *in vitro* were compared between these two genotypes with/without $Ca^{2+}$ inhibitors or ROS scavenger treatments. Differences in ANPC proliferation and differentiation capabilities *in vivo* between the two genotypes were evaluated using Ki-67 and Doublecortin (DCX) immunofluorescence respectively.

*Results*: Compared to WT ANPCs, YAC128 ANPCs had significantly enhanced cell proliferation, migration and neuronal differentiation *in vitro*, accompanied by increased $Ca^{2+}$ and ROS signals. Raised proliferation and migration in YAC128 ANPCs were abolished by $Ca^{2+}$ signalling antagonists and ROS scavenging. However, *in vivo*, HD ANPCs failed to show any elevated proliferation or differentiation.

*Conclusions*: Increased $Ca^{2+}$ signalling and higher level of ROS conferred HD ANPC enhancement of proliferation and migration potentials. However, the *in vivo* micro-environment did not support endogenous ANPCs to respond appropriately to neuronal loss in these YAC128 mouse brains.

Correspondence: Tie-Shan Tang, State Key Laboratory of Biomembrane and Membrane Biotechnology, Institute of Zoology, Chinese Academy of Sciences, Chaoyang District, Beijing 100101, China. Tel.: +86 10 64807296; Fax: +86 10 64807313; E-mail: tangtsh@ioz.ac.cn; and Sheng Yao, Department of Neurology, Navy General Hospital, Beijing 100048, China. Tel: +86-10-68780622; E-mail: bjyaosheng@sina.com

## Introduction

Throughout adulthood, mammalian neurogenesis mainly occurs in two regions: the subventricular zone (SVZ) of brain lateral ventricles and subgranular zone (SGZ) of the hippocampal dentate gyrus (DG) (1,2). Newborn neurons form functional connections with existing circuitry to maintain and reorganize the olfactory bulb (3–5) and contribute to hippocampal-dependent memory and behaviour (6–8). Importantly, neurogenesis can be up-regulated by a variety of stimuli such as occurrence of seizures, either ischaemic or by stroke (9–12). These findings spark considerable interest in endogenous cell repair strategies, and the adult neural progenitor cells (ANPCs) have been proposed to be an endogenous source of cells for treatment of neurodegenerative diseases (13,14). Neurogenesis has been widely studied in a number of neurodegenerative disorders including Alzheimer's disease (15–17), Parkinson's disease (18–20) and Huntington's disease (HD) (21–24).

HD is an inherited human neurodegenerative disorder caused by hugely expanded CAG repeats in the huntingtin (*HTT*) gene, characterized by neuronal cell death in discrete brain regions, resulting in movement disorders, psychiatric disturbance, and cognitive decline (25,26). The striatum is the brain structure primarily affected, although other areas can also be affected in patients with advanced HD (27). Due to close proximity of the SVZ to the striatum, neurogenesis in the SVZ has consistently been

studied in HD transgenic mouse models, as well as in HD patients. Several lines of evidence have demonstrated normal ANPC proliferation in the SVZ in multiple HD transgenic mouse brains *in vivo* (21–24), while others have shown impaired proliferation capacity of neural stem cells (NSCs) isolated/cultured from embryonic HD mouse brains *in vitro* (28,29). Interestingly, in human post-mortem HD brains, increase has been found in ANPC proliferation in the SVZ, specially in patients with advanced HD (30). To date, there has not been any clear explanation for these conflicting observations.

Neurogenesis is a complex process which includes proliferation, migration and differentiation, and can be affected by intrinsic properties of endogenous neural progenitor cells (NPCs) and the micro-environment in which they reside *in vivo*. YAC128 HD mouse model animals express the full-length human mutant *HTT* gene with 128 CAG repeats, and faithfully recapitulates many features of the human condition (31,32). In the present study, to determine whether intrinsic properties of ANPCs were changed in response to HD, we examined proliferation, migration and neuronal differentiation capacities of ANPCs isolated from SVZ regions of age-matched WT and YAC128 HD mouse brains, *in vitro*. Somewhat surprisingly, we found that proliferation, migration and neuronal differentiation significantly increased in YAC128 ANPCs, and that enhanced $Ca^{2+}$ and ROS signals were essential for enhancements of proliferation and migration in YAC128 ANPCs. Mutant HTT protein-triggered elevated $Ca^{2+}$ and ROS signalling have been previously reported to be harmful to mature neurons including striatal medium spiny neurons (MSNs) in HD (33–39). Thus, in contrast to their toxicities to mature neurons in HD, elevated $Ca^{2+}$ and ROS signalling seem to deliver increased capabilities of proliferation and migration to HD ANPCs. Interestingly, unlike results *in vitro*, YAC128 HD mouse brains had similar levels of ANPC proliferation and differentiation to WT SVZ ones, *in vivo*, indicating that the micro-environment in which the ANPCs were organized was the key limiting factor for adult neurogenesis in YAC128 HD mouse brains, rather than intrinsic proliferation and differentiation properties of the cells. Thus, to promote endogenous neurogenesis to counteract striatal neurodegeneration in HD brains, liberating ANPCs from their constrained micro-environment is a key approach that should be considered.

## Materials and methods

### *Isolation and culture of adult neural progenitor cells*

YAC128 HD transgenic mice were obtained from the Jackson Laboratory (Bar Harbor, ME, USA). Generation and breeding of transgenic YAC128 HD mice (FVBN/NJ background strain) have previously been described (31). All animal experiments were reviewed and approved by our Institute of Zoology Institutional Animal Care and Use Committee and were conducted according to the committee's guidelines. 4-month-old wild type and YAC128 mice (FVB strain) were sacrificed by decapitation. Subventricular zones from individual animals was dissociated with accutase (Millipore, Temecula, CA, USA) for 10 min at 37 °C, and mechanically dissociated using a fire-polished 1000 μl plastic tip. After centrifugation, cells were re-suspended in growth medium consisting of neurobasal medium, 2% B27 supplement without vitamin A, 1% glutamax, 1 × penicillin/streptomycin (all from Invitrogen, Carlsbad, CA, USA) and 20 ng/ml of both epidermal growth factor (EGF) and basic fibroblast growth factor (FGF2) (Peprotech, Rocky Hill, NJ, USA). Cells were plated in growth medium either on to six-well uncoated plastic plates for floating spheres, or on to poly-L-ornithine-coated plastic plates for monolayer cultures. Half the volume of each culture medium was changed every 2 days, and cells were passaged every 4–6 days with accutase. After expanding and propagating them for at least 14 passages, monolayer cultured cells were fixed and probed with antibodies against Nestin (1:200; Millipore) and SOX2 (1:200; Abcam, London, UK).

### *Adult neural progenitor cell differentiation*

Adult neural progenitor cells were induced to differentiate after plating on poly-L-ornithine-coated glass coverslips. The detailed procedure was adapted from a protocol previously described, which requires withdrawal of EGF and slow reduction of FGF2 while introducing and increasing brain-derived neurotrophic factor (BDNF) (40). Half the medium was exchanged after 72 h incubation in respective defined media. Cells were then fixed and probed with antibodies against microtubule-associated protein (MAP2) (1:400; Chemicon, Temecula, CA, USA) and glial fibrillar acidic protein (GFAP) (1:400; Chemicon). Soma area neurite length of $MAP2^+$ cells were measured using Image-J software.

### *Cell proliferation assays*

Self-renewal was first assessed by dissociating neurospheres into single cells and re-culturing them at low density of 1000 cells per well, in 24-well plates. Size of secondary spheres after 8 days culture was measured using Image-J software. Neurospheres with diameters >40 μm were assessed.

Growth curve experiments were also used to evaluate capability for cell proliferation. $5 \times 10^4$ cells per well were seeded in poly-L-ornithine-coated six-well plates in 2 ml growth medium, with or without testing agents (100 μM glutamate, 50 μM 2-APB, 1 mM NAC, 1 μM/2 μM U73122), and each sample was plated in triplicate. Cell number was counted after 0, 2 and 4 days culture. At each time point, cells were dissociated using accutase then resuspended in growth medium. Aliquots of cells were incubated in trypan blue (Sigma, St. Louis, MO, USA) then counted with the aid of a haemocytometer.

Proliferation was further determined using 5-bromodeoxyuridine (BrdU) incorporation. Dissociated cells were plated on glass coverslips coated with poly-L-ornithine (0.015 mg/ml) and cultured for 48 h. Cells were incubated for 5 h with 10 μM BrdU, and then fixed and washed. DNA was denatured by incubating the cells in 1 N HCl for 45 min at room temperature. Cells were washed and blocked with 10% bovine serum albumin for 60 min at room temperature, and primary mouse anti-BrdU antibody (1:200, BD, San Jose, CA, USA) was applied and incubated for 60 min at 37 °C followed by goat anti-mouse Alexa 546 antibody (1:500, Invitrogen). Nuclei were stained with 10 μg/ml Hoechst 33342 (Sigma). Images were acquired using a Leica inverted fluorescence microscope.

### *Migration assay*

Neurospheres with similar diameters were selected and plated on poly-L-ornithine-coated six-well culture plates containing neurobasal medium supplemented with 2% B27 with or without NAC (5 mM) or 2-APB (50 μM) or U73122 (2 μM/5 μM) for 12 or 24 h. Cell migration was evaluated by measuring distances ANPCs had migrated from edges of neurospheres towards exernal borders.

### *$Ca^{2+}$ imaging*

Intracellular $Ca^{2+}$ measurements were performed on cells bathed in imaging buffer comprised of 140 mM NaCl, 5 mM KCl, 1 mM $MgCl_2$, 2 mM $CaCl_2$, 10 mM glucose and 20 mM HEPES (pH 7.3). Cells were loaded with 4 μM of Fura-2 AM (Invitrogen) for 40 min at room temperature (RT), then allowed further 10 min after washing to de-ester the dye before imaging. Images were captured using a Nikon inverted microscope (Eclipse Ti) and ×40 magnification oil-immersion objective lens (N.A. = 1.40). Cells were alternatively excited at 340 nm and 380 nm, using a single-band multi-exciter filter set (FURA2-C-000, BrightLine; Semrock, Rochester, New York, USA), emissions were collected through a 409 nm single-edge dichroic beam splitter (BrightLine, Semrock) and 510/84 nm single-band emitter (BrightLine, Semrock). Images were collected every 2 seconds for the duration of the experiment. Intracellular $Ca^{2+}$ concentration ($[Ca^{2+}]_i$) within single cells was reported as ratio of the 510 nm emission excited at 340 and 380 nm (340/380). Glutamate (100 nM) was added at 100 s to induce calcium signaling and changes in $Ca^{2+}$ levels were monitored for 400 s. To verify efficiency of 2-APB (50 μM) and U73122 (2 μM), these drugs were added at 60 s before 100 μM glutamate was added at 200 s.

### *ROS measurement*

Intracellular ROS level was assessed using 2′,7′-dichlorodihydrofluorescein diacetate (DCFH-DA) (Beyotime, Shanghai, China), which can be hydrolysed to 2′,7′-dichlorodihydrofluorescein (DCFH) by esterases; then DCFH is oxidized by ROS in the cells, yielding 2′,7′-dichlorofluorescein (DCF). After treatment with NAC (1 mM, 18 h; 5 mM, 4 h), cells were washed with neurobasal medium, incubated in 10 μM of DCFH-DA at 37 °C for 30 min, and washed twice in neurobasal medium. Then they were resuspended into a single cell suspension using accutase, and analysed by flow cytometry. To detect mitochondrial superoxide production, monolayer cultured cells were treated for 15 min at 37 °C with 5 μM of MitoSOX™ Red (Molecular Probes; Invitrogen), and washed three times, digested with accutase, collected by centrifugation, and analysed by flow cytometry. Flow cytometric analysis was performes immediately after dye treatment. All measurements were repeated at least three times.

### *Immunofluorescence*

To examine cell proliferation and differentiation *in vivo*, a separate set of 4-month- (4 WT, 5 YAC128) and 18-month- (7 WT, 6 YAC128) old mice were sacrificed. Mice were deeply anaesthetized with chloral hydrate, perfused transcardially with PBS and fixed with 4% paraformaldehyde. Brains were excised, post-fixed overnight at 4 °C, and transferred to 30% sucrose. 25 μM coronal brain sections were processed for detection of Ki-67-positive cells and DCX-positive cells. After rinsing briefly in PBS, sections were treated for 2 h in 10% donkey serum and 0.3% Triton X-100 in PBS then incubated in rabbit polyclonal antibody against Ki-67 (1:200, Abcam) or a rabbit polyclonal antibody against DCX (1:200, Abcam) in PBS containing 5% donkey serum, for 12 hours at 4 °C. Sections were then rinsed three times in PBST (PBS plus 0.3% tween-20) and

incubated for 2 hours in Alexa Fluor 488-labelled donkey anti-rabbit IgG antibody (1:1000; Invitrogen). Hoechst33342 (10 μg/ml;, Invitrogen) labelled the positions of cell nuclei. Fluorescence-stained sections were analysed using a confocal laser-scanning microscope (Carl Zeiss LSM510).

### *Data collection and analyses*

In experiments when cell counts or measurements were involved, a naive person collected all images, to minimize potential observer bias. All such experiments were repeated at least three times and a representative experiment is presented here. Data are shown as mean ± SE, statistical comparisons were made using the independent samples *t*-test, and significance level was set at 5%.

## Results

### *Characteristics of NPCs isolated from adult mouse SVZ*

In our study, NPCs were isolated from SVZs of 4-month-old WT and YAC128 mice. NPCs were grown as either neurospheres in non-coated plates (Fig. 1a) or monolayer cultures on poly-L-ornithine-coated dishes (Fig. 1b) in the presence of EGF and FGF2. After expanding and propagating cells for at least 14 passages, they uniformly expressed Nestin and SOX2 (Fig. 1c), markers typically found in uncommitted neural stem cells (41,42), indicating that our ANPCs maintained stem cell characteristics over the culture period and that these cell populations were highly homogeneous.

ANPCs were plated as monolayers and differentiated using a previously described protocol (40), in which EGF was withdrawn and FGF2 concentrations reduced while BDNF was increased. Differentiated cells were stained for lineage-specific differentiation markers MAP2 (for neurons) and GFAP (for astrocytes) (Fig. 1d), demonstrating multipotencies of ANPCs isolated from SVZ regions of adult WT and YAC128 mouse brains.

### *YAC128 ANPCs had higher cell proliferation, migration and neuronal differentiation capabilities*

One major property of stem cell is self-renewal (43), thus we first compared proliferation capabilities between WT and YAC128 ANPCs; neurosphere formation was evaluated as an indicator of this. To minimize effects of cell aggregation during growth of neurospheres, ANPCs were plated at low density. After 8 days of culture, diameters of neurospheres were measured. As shown in Fig. 2a, there was significant increase in size of the spheres, detected in YAC128 ANPCs compared to WT cells, suggesting that YAC128 ANPCs had much higher proliferative potential than WT ANPCs. This result was further confirmed by growth curve experimentation. YAC128 ANPCs had a much higher growth rates than WT ANPCs (Fig. 2b), confirming their higher potential for self-renewal in HD ANPCs. Furthermore, percentages of BrdU-positive cells in YAC128 ANPCs was significantly higher than that in WT cells as shown by BrdU incorporation assay (Fig. 2c,d).

To determine whether there was any difference in mobility between WT and YAC128 ANPCs, an *in vitro* migration assay was employed. After culturing on poly-ornithine-coated plates for 12 h, ANPCs from neurospheres migrated radially outwards (Fig. 2e). Distances from edges of neurospheres to borders to which the ANPCs migrated were measured to evaluate cell migration. Statistics analysis indicated that YAC128 ANPCs migrated significantly faster than WT ANPCs (Fig. 2f).

We next compared potentials for neuronal differentiation between WT and YAC128 ANPCs *in vitro*. ANPCs were differentiated using a previously described protocol (40). As shown in Figs. 1d and 2g, both genotypes of ANPCs were able to differentiate into neurons ($MAP2^+$). Percentages of $MAP2^+$ cells were then quantified by normalizing total $MAP2^+$ cells to total $Hoechst33342^+$ cells. YAC128 ANPCs differentiated for 21 days had significantly higher percentages of $MAP2^+$ cells compared to WT ANPCs of identical passage and differentiation times (Figs. 1d,2g). Moreover, neurite length of differentiated YAC128 $MAP2^+$ cells was significantly longer than that of WT $MAP2^+$ cells (Fig. 2i). No significant difference was detected in soma area between YAC128 and WT neuronal like cells (Fig. 2h). Thus, YAC128 HD ANPCs were able to differentiate into greater numbers of neurons with longer neurites compared to WT ANPCs, indicating enhanced neuronal differentiation capacities in HD ANPCs.

### *ANPCs exhibited enhanced $Ca^{2+}$ signals*

It has already been demonstrated that polyQ expansion in HTT induces enhanced $Ca^{2+}$ signalling in HD MSNs

**Figure 1. ANPC cultures and monolayer ANPC differentiation *in vitro*.** (a) ANPCs were grown as neurospheres in a non-coated six-well plastic plate. Scale bar: 250 μm. (b) ANPCs were grown as monolayers in poly-ornithine-coated six-well plastic plates. Scale bar: 250 μm. (c) Monolayer ANPCs were stained with Nestin (green) and SOX2 (red). Scale bar: 50 μm. (d) Monolayer ANPCs were able to differentiate into neurons (MAP2, red) and astrocytes (GFAP, green). Scale bar: 50 μm.

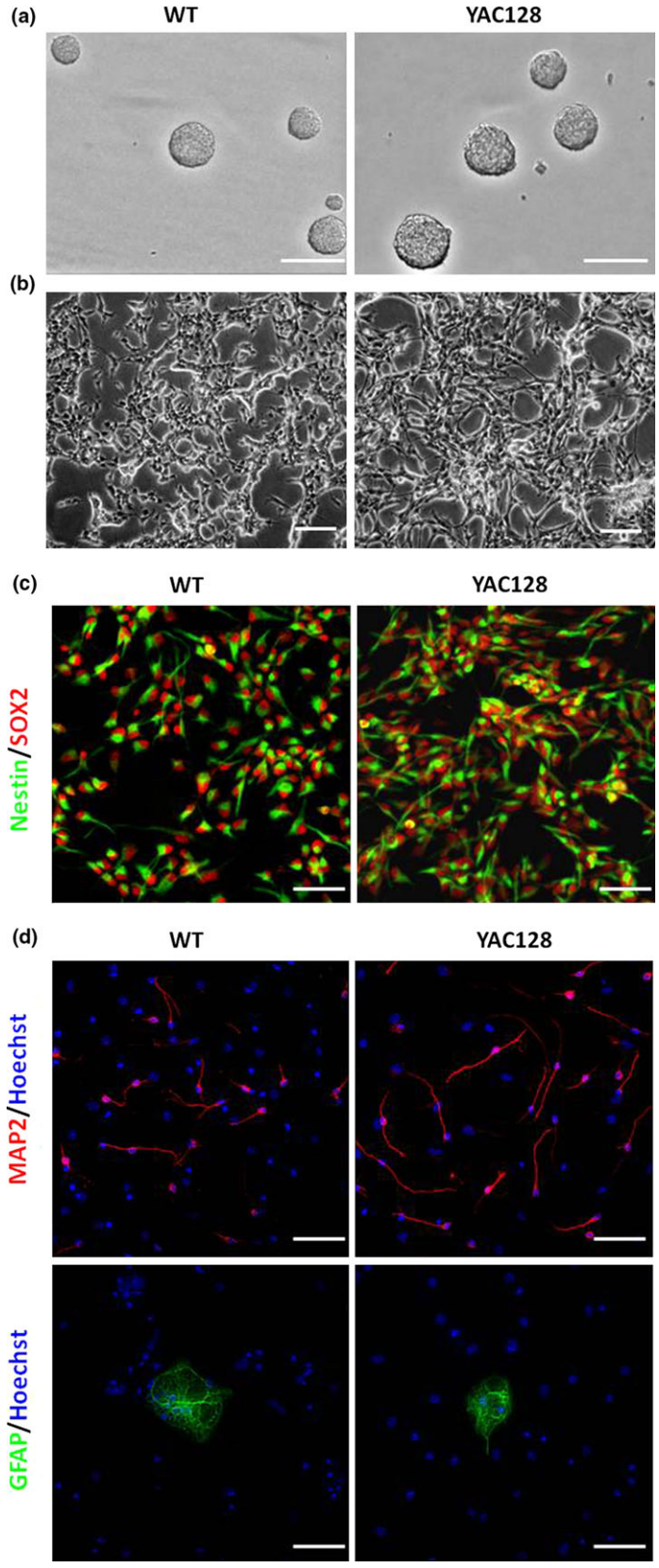

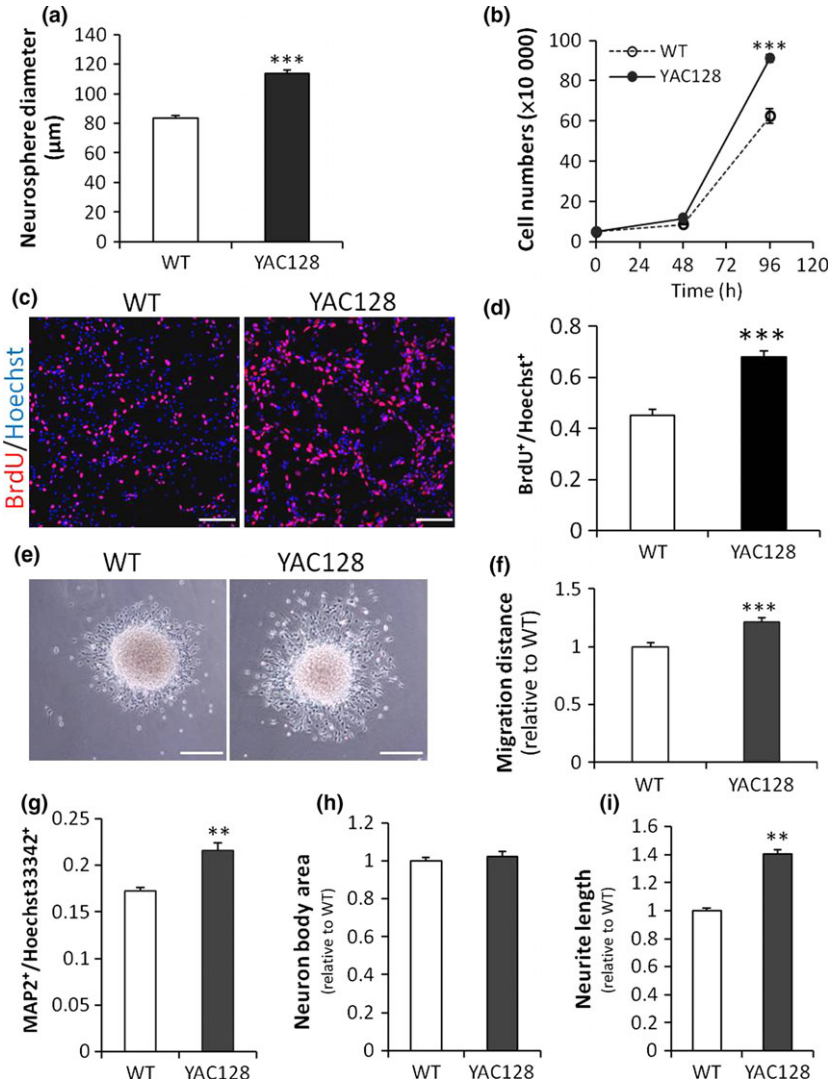


**Figure 2. ANPCs derived from SVZ of HD mouse brain exhibit increased proliferation, migration and neurogenic differentiation compared with that of WT control**. (a) Neurosphere assay. The size of neurospheres were determined after 8-day culture *in vitro* ($n$ = 70 neurospheres per group, ***$P < 0.001$). (b) YAC128 HD ANPCs had a much higher rate of growth compared with the WT control ($n$ = 3, ***$P < 0.001$). (c,d) BrdU incorporation assay. The percentage of BrdU-positive cells in YAC128 ANPCs was significantly higher than that in WT cells ($n$ = 6, ***$P < 0.001$). Scale bar: 100 μm. (e) Neurospheres cultured on poly-L-ornithine dishes migrated outwards radially. Scale bar: 500 μm. (f) The radial migration distance of YAC128 HD neurospheres were significantly increased compared with the WT control after 12-hour cultivation ($n$ = 40 neurospheres per group, ***$P < 0.001$). (g) The percentage of neuronal cells ($MAP2^+$) was quantified by normalizing the total $MAP2^+$ cells to the total $Hoechst33342^+$ cells after 21-day differentiation ($n$ = 3, **$P < 0.01$). (h) Quantification of the soma area of neurons derived from WT and YAC128 ANPCs ($n$ = 50 neurons per group). (i) Neurite lengths of $MAP2^+$ cells derived from WT and YAC128 ANPCs were measured. Independent $t$-test showed a significant increase in neurite length in YAC128 neurons compared with WT neurons ($n$ = 50 neurons per group, **$P < 0.01$). Data were shown as the mean ± SE.

(33–37). To investigate whether this also exists in ANPCs, we compared glutamate-induced $Ca^{2+}$ signalling between WT and YAC128 ANPCs. Intracellular $Ca^{2+}$ concentration was monitored using Fura-2 imaging, and data are presented as 340/380 ratios (Fig. 3a–c). On average, basal $Ca^{2+}$ levels before glutamate application were not significantly different from each other between genotypes of ANPC (Fig. 3a). Treatment with 100 nM glutamate caused significantly higher amplitude of transient cellular $Ca^{2+}$ in YAC128 ANPCs over WT ANPCs (Fig. 3a–b). To quantify amounts of $Ca^{2+}$ loaded into cytoplasm during glutamate stimulation, we calculated areas (ratio*s) below transient $Ca^{2+}$ traces. Significantly higher amounts of $Ca^{2+}$ were loaded into the cytoplasm in YAC128 ANPCs than WT ANPCs (Fig. 3c). Similarly, treatment with 100 μM glutamate also caused significantly

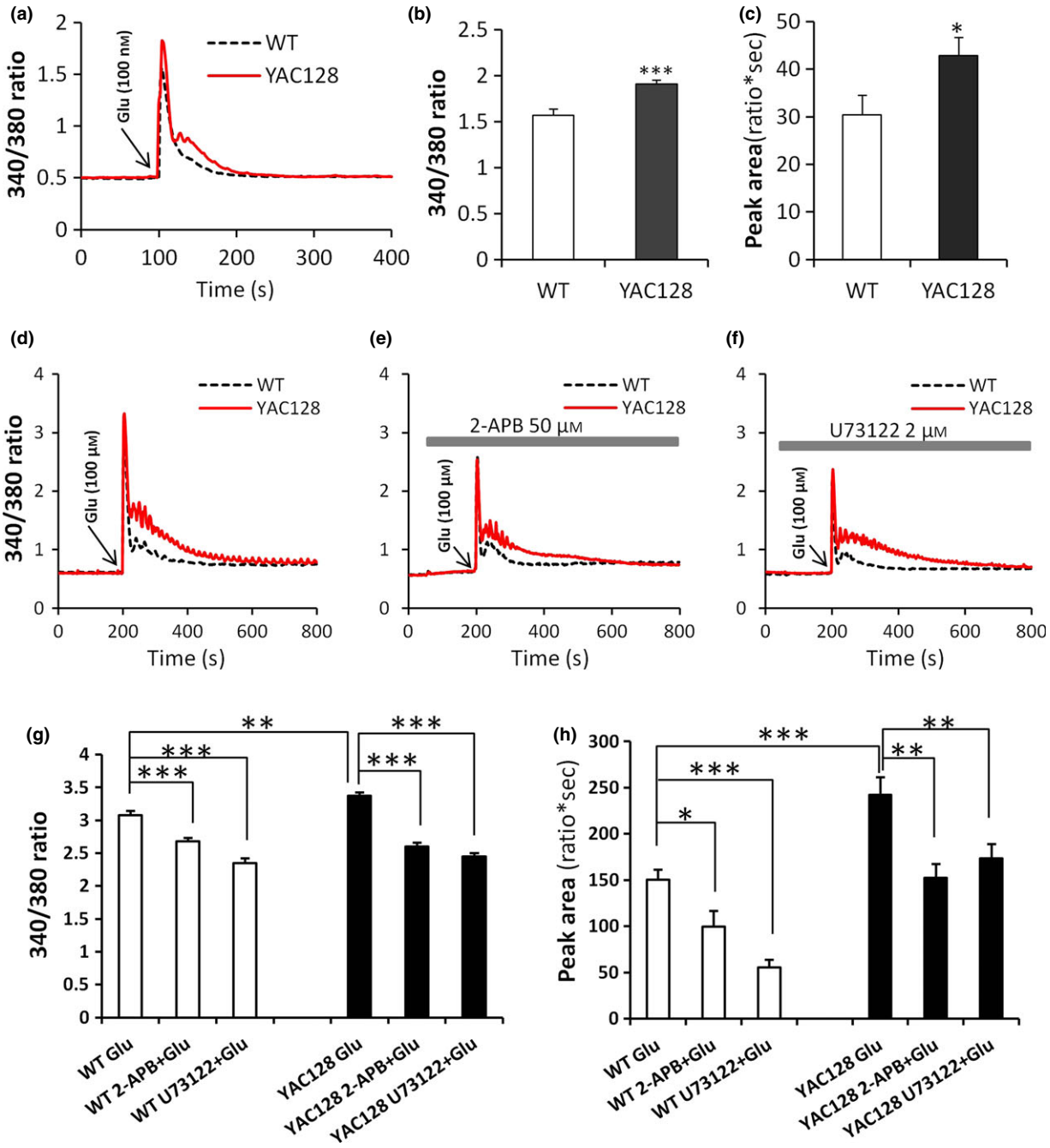


**Figure 3. YAC128 ANPCs exhibit increased $Ca^{2+}$ signalling compared with the WT controls**. (a) 100 nM glutamate-induced $Ca^{2+}$ signals in ANPCs from the WT and YAC128 mouse brains. Intracellular $Ca^{2+}$ concentration ($[Ca^{2+}]_i$) was presented as a 340/380 Fura-2 ratio. The average 340/380 values (mean ± SE) were shown for WT ($n$ = 23) and YAC128 ($n$ = 30) ANPCs. Both peak values (b) and peak areas (c) were significantly higher in YAC128 ANPCs than in the WT controls (*$P$ < 0.05, ***$P$ < 0.001). (d) The 100 μM glutamate-induced $Ca^{2+}$ signals in ANPCs from the WT and YAC128 mouse brains. Both peak values (g) and peak areas (h) were significantly higher in YAC128 ($n$ = 21) ANPCs than in the WT ($n$ = 23) controls (**$P$ < 0.01, ***$P$ < 0.001). The 100 μM glutamate-induced $[Ca^{2+}]_i$ transients in WT and YAC128 ANPCs were significantly reduced in the presence of the InsP3R blocker 2-APB (50 μM) (e) and PLC inhibitor U73122 (2 μM) (f). (g) Effect of 2-APB and U73122 on the peak value of $[Ca^{2+}]_i$ in WT and YAC128 ANPCs in response to 100 μM glutamate. Pre-treatment with 2-APB and U73122 significantly decreased the peak value of $[Ca^{2+}]_i$ in both WT ($n$ = 20 for 2-APB and $n$ = 23 for U73122) and YAC128 ANPCs ($n$ = 26 for 2-APB and $n$ = 22 for U73122) when compared with the control group (***$P$ < 0.001). (h) Effect of 2-APB and U73122 on the peak area of $[Ca^{2+}]_i$ in WT and YAC128 ANPCs in response to 100 μM glutamate. Pre-treatment with 2-APB and U73122 significantly decreased the peak area of $[Ca^{2+}]_i$ in both WT and YAC128 ANPCs when compared with the control group (*$P$ < 0.05, **$P$ < 0.01,***$P$ < 0.001).

higher transient $Ca^{2+}$ and more $Ca^{2+}$ load in YAC128 ANPCs than in WT ANPCs (Fig. 3d,3g–h). Additionally, both 2-APB and U73122 significantly reduced $Ca^{2+}$ levels in both ANPC genotypes (Fig. 3d–h).

### *Enhanced $Ca^{2+}$ signals were required for increased proliferation and migration of HD ANPCs*

$Ca^{2+}$ signalling has previously been discussed in regulating neural stem/progenitor cell proliferation (44–47) and migration (48–51). In our study, we first evaluated effects of glutamate-induced $Ca^{2+}$ signalling on ANPC proliferation in each genotype. After incubation with 100 μM glutamate for 4 days, both genotypes underwent significant increases in proliferative rate compared to their control groups, and YAC128 HD ANPCs proliferated more rapidly than WT ANPCs (Fig. 4a), indicating that elevation of cellular $Ca^{2+}$ lead to higher ANPC growth rate. Thus, increased proliferation of YAC128 ANPCs could be associated with their enhanced $Ca^{2+}$ signalling. To confirm this, $Ca^{2+}$ signalling was inhibited either by 2-APB [a cell-permeable $IP_3R$ inhibitor (52)] or U73122 [a specific PLC inhibitor (53)], and cell proliferation was assessed under these conditions respectively. Treatment with 50 μM 2-APB significantly reduced cell proliferation in both WT and YAC128 HD ANPCs, and HD ANPCs no longer exhibited any proliferative advantage (Fig. 4b). Similar results were obtained when $Ca^{2+}$ signalling in ANPCs was inhibited by U73122 (Fig. 4c). When treating with 2 μM of U73122, YAC128 ANPCs exhibited similar cell proliferation rates as WT ANPCs (Fig. 4c). These results indicate that increased proliferation of YAC128 ANPCs was calcium-dependent. In addition, treatments with 2-APB and U73122 did not cause significant cell death, excluding the possibility that inhibition of proliferation was due to increased cell death. (Fig. S1).

$Ca^{2+}$ signalling has also been shown to play a role in neuronal motility, for example in migration of neural precursors, as well as elongation and branching of neurites (54). To test whether increased migration in

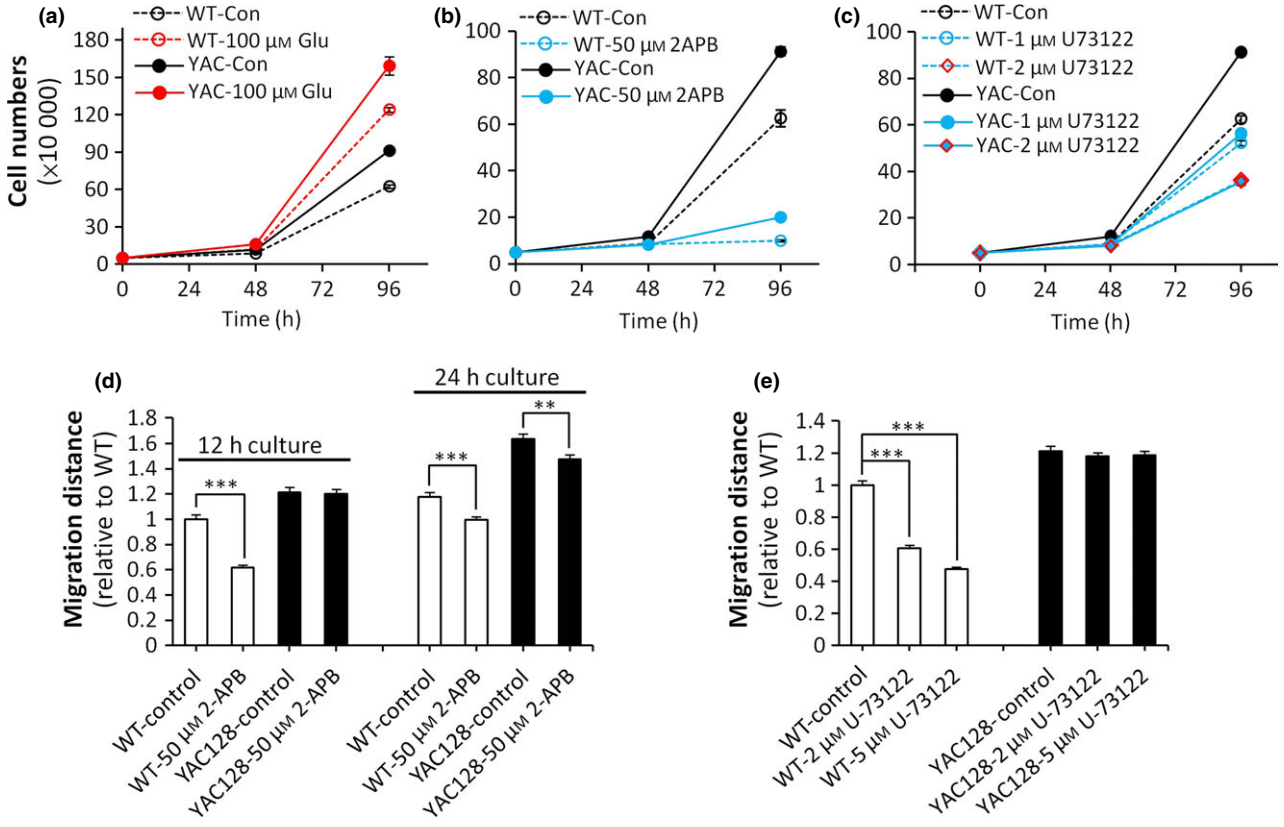


**Figure 4. Enhanced $Ca^{2+}$ signals are required for the enhanced proliferation and migration in YAC128 HD ANPCs compared with WT ANPCs**. (a) Glutamate promoted the proliferation of both WT and YAC128 ANPCs. 2-APB, an inhibitor of intracellular $Ca^{2+}$ signal, strongly inhibited the proliferation (b) and migration (c) U-73122, a PLC blocker, dose-dependently inhibited the proliferation of ANPCs from WT and YAC128 mice. (d) of both WT ANPCs and YAC128 ANPCs (**$P < 0.01$; ***$P < 0.001$). WT ANPCs were more sensitive to 2-APB than YAC128 ANPCs in cell migration. (e) U-73122 inhibited the migration of WT ANPCs significantly (***$P < 0.001$), while the migration of YAC128 ANPCs was not affected by U-73122. Data were presented as mean ± SE.

YAC128 ANPCs could be attributed to enhanced $Ca^{2+}$ signalling, we compared migration capabilities between WT and YAC128 ANPCs with/without $Ca^{2+}$ signalling inhibitors. Neurospheres with similar diameters were plated into poly-L-ornithine-coated dishes, cultured for 12 or 24 h with or without $Ca^{2+}$ signalling inhibitors. As shown in Fig. 4d, 12 h after initiation of culture, 50 μM of 2-APB significantly inhibited radial migration of both WT and YAC128 ANPCs, in a time-dependent manner. Similar results were obtained using U73122 treatment (Fig. 4e). Both $Ca^{2+}$ signalling inhibitors (2-APB and U73122) were very effective in reducing migration of WT ANPCs but less of YAC128 ANPCs. These results indicated that reduction in $Ca^{2+}$ signalling slowed ANPC migration, and relatively higher levels of $Ca^{2+}$ signalling were essential for rapid migration. YAC128 ANPCs, which had much higher levels of $Ca^{2+}$ signalling compared to WT ANPCs, may not be so sensitive to reduction in $Ca^{2+}$ signalling during migration.

Taken together, these data indicate that enhanced $Ca^{2+}$ signaling is essential for increased proliferation and migration capacities of YAC128 ANPCs.

### *YAC128 ANPCs had increased levels of reactive oxygen species*

Marked changes in levels of reactive oxygen species have previously been identified in HD brain and in HD cell models (29,38,55–57). Primary cultured medium spiny neurons (MSNs) from YAC128 neonatal mouse brains have higher levels of reactive oxygen species (ROS) than WT cortical neurons (39). To determine if changes in ROS levels occurred in YAC128 ANPCs, ROS levels in live cells were measured by using DCFH-DA. This is hydrolysed by esterases to DCFH, and DCFH is oxidized by ROS in the cells, yielding DCF. We found significant increase in DCF fluorescence in YAC128 compared to WT cells (Fig. 5a). Given the pivotal role of mitochondria in generation of ROS (58), mitochondrial ROS (mt-ROS) were monitored by MitoSOX™ Red (Molecular Probes). Levels of mt-ROS in YAC128 ANPCs were also significantly higher than in WT controls (Fig. 5b).

### *Enhanced ROS signals were required for increased proliferation and migration of YAC128 ANPCs*

ROS may play roles in regulating neural progenitor cell proliferation (59–62). Thus, to determine potential relationships between enhanced ROS and increased proliferation in HD ANPCs, cells were cultured at the same density in the presence or absence of the ROS scavenger N-acetylcysteine (NAC) and analysed for changes in proliferation. As expected, NAC significantly reduced cellular ROS levels of both WT and YAC128 ANPCs (Fig. 6a). In the absence of NAC, YAC128 ANPCs had more rapid proliferation than WT ANPCs (Fig. 6b), while in the presence of 1 mM NAC [which could not cause significant cell death during treatment (Fig. S1)], both WT and YAC128 ANPCs failed to proliferate (Fig. 6b), demonstrating ROS to be an essential signal for maintenance of ANPC self-renewal.

ROS has also been linked to cell migration (63–65). Next, we investigated the relationship between redox state and ANPC migration. Chelating cellular ROS by NAC strongly inhibited migration of both WT and YAC128 HD ANPCs (Fig. 6c), indicating that ROS signalling is also required for ANPCs migration.

In summary, these observations indicated that increased proliferation and migration in YAC128 ANPCs were critically depended on enhanced ROS signalling.

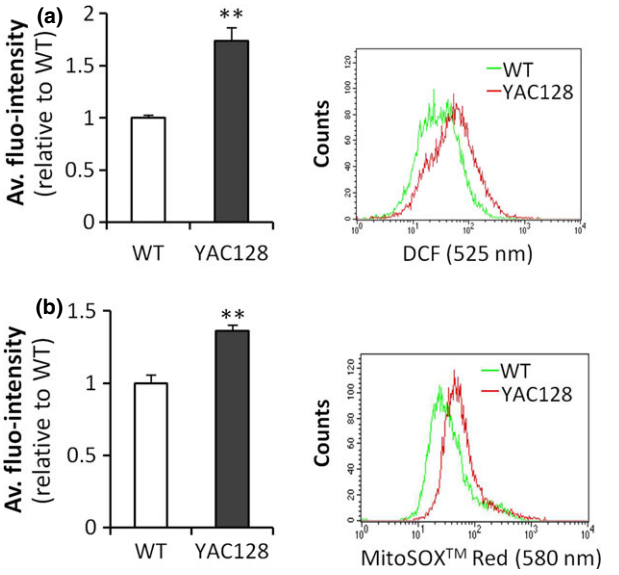


**Figure 5. YAC128 ANPCs show enhanced ROS signals**. (a) DCF fluorescence was used as a marker of ROS and was measured in live cells with flow cytometry. Left, measurements of ROS in YAC128 ANPCs and WT ANPCs. YAC128 ANPCs had higher levels of ROS compared with WT controls. Right, scatter plot histogram of a representative experiment. (b) MitoSOX™ Red fluorescence was used as an indicator of mitochondrial superoxide and was measured in live cells with flow cytometry. Left, measurement of mitochondrial superoxide in YAC128 ANPCs compared to WT ANPCs. YAC128 ANPCs had higher levels of mitochrondrial ROS compared with WT control. Right: scatter plot histogram of a representative experiment. Data were presented as mean ± SE ($n$ = 3, $^{**}P < 0.01$).

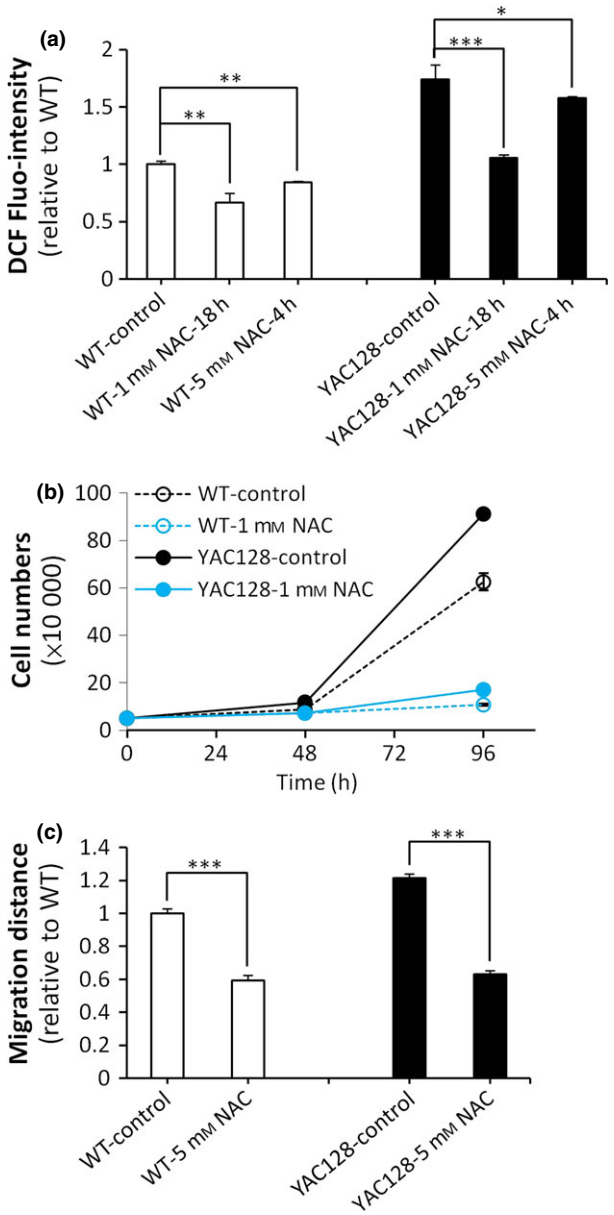


**Figure 6. Increased ROS signals are required for enhanced proliferation and migration in YAC128 ANPCs compared with WT ANPCs**. (a) Measurement of ROS levels in YAC128 and WT ANPCs pre-treated with NAC, a ROS scavenger. NAC was able to decrease ROS signal significantly in both YAC128 and WT ANPCs ($n = 3$, $^*P < 0.05$; $^{**}P < 0.01$; $^{***}P < 0.001$). (b) NAC inhibited the proliferation of YAC128 and WT ANPCs. (c) NAC inhibited the migration of YAC128 and WT ANPCs significantly ($n = 40$ neuropheres per group, $^{***}P < 0.001$). Data were presented as mean ± SE.

### *YAC128 ANPCs exhibited normal proliferation and differentiation in the subventricular zone of mouse brains*

Our experiments provide compelling evidence that YAC128 ANPCs manifest $Ca^{2+}$/ROS signalling-dependent enhancement in proliferation and migration *in vitro*. To discover any substantiation of our *in vitro* observations, experiments were undertaken to address whether ANPCs in HD mouse brains would have higher rates of cell proliferation than that in WT brains, *in vivo*. Antibody to Ki-67, a nuclear antigen expressed during all stages of the cell cycle except G0, was used to label proliferating cells (Fig. 7a). There were no significant differences in cell proliferation between YAC128 and WT mouse brains at either 4 or 18 months of age, although there was significantly age-dependent decline in numbers of proliferating cells in the SVZ of both genotypes (Fig. 7b). These results were consistent with previous reports (24), that proliferation of ANPCs appears to be no more than normal in SVZ of YAC128 HD mouse brains compared to WT brains. Moreover, numbers of immature neurons in the SVZ were also quantified by immunofluorescence for DCX (Fig. 7c). YAC128 mice displayed similar numbers of DCX-positive cells in the SVZ as their WT controls (Fig 7d). We propose that micro-environment in the SVZ constrained proliferation and differentiation capacities of HD ANPCs *in vivo*.

## Discussion

To evaluate intrinsic capacities of adult neural progenitor cells for proliferation and neuronal differentiation subjected to Huntington's disease conditions, we isolated neural progenitor cells from adult brains of mice expressing endogenous levels of full-length human mutant HTT protein (YAC128). Both WT and YAC128 ANPCs were able to differentiate to both neurons and astrocytes. Compared to wild-type ANPCs, YAC128 HDs manifested increased cell proliferation, migration, and neuronal differentiation capacities, accompanied by enhanced $Ca^{2+}$ signalling and higher levels of intracellular reactive oxygen species (ROS). Here, we provide compelling evidence to demonstrate that enhanced $Ca^{2+}$ and ROS signals (which are detrimental to mature medium spiny neurons), are essential for this intrinsic change in properties in HD ANPCs. This is the first report that mutant HTT protein triggers $Ca^{2+}$ and ROS signalling-dependent enhancement of proliferation and migration in HD ANPCs. Interestingly, increased proliferation and neuronal differentiation of HD ANPCs was largely constrained by the *in vivo* micro-environment in mouse brains. Thus, our results also point to a new direction for development of cell-based therapeutic strategies in HD: remodelling the *in vivo* micro-environment is the key to liberate ANPC potential for promoting endogenous neurogenesis.

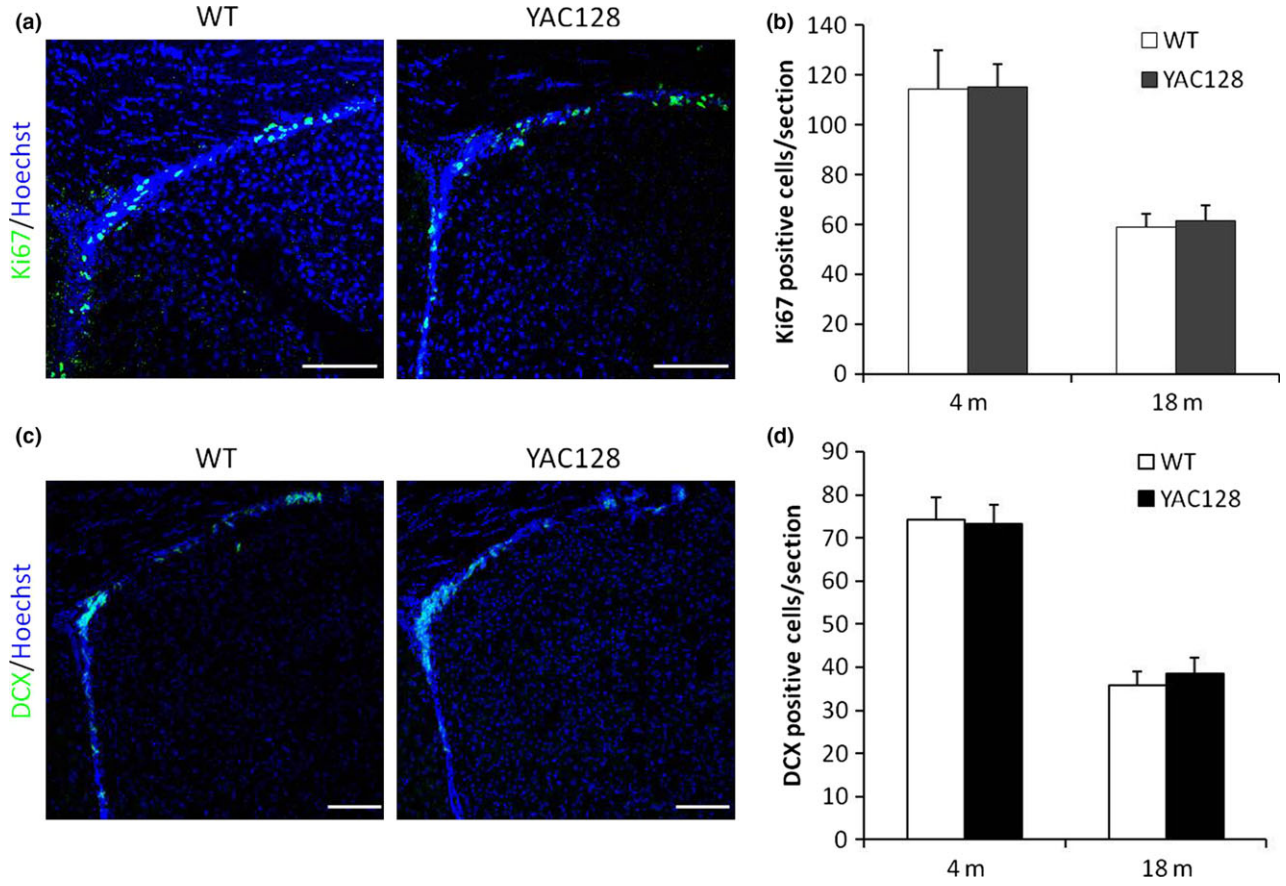


**Figure 7. YAC128 HD mice show similar levels of ANPC proliferation and differentiation as WT mice in SVZ**. (a) Endogenous ANPC proliferation in the SVZ was assessed by immunofluorescence for cell cycle marker Ki67. (b) Statistic analysis of Ki-67-positive cells in SVZ. No significant difference between the genotypes in the number of Ki-67-positive cells was observed. (c) Endogenous ANPC neuronal differentiation in the SVZ was assessed by DCX immunofluorescence. (d) Statistic analysis of DCX-positive cells in SVZ. No significant difference between the genotypes in the number of DCX-positive cells was observed. Data were presented as mean ± SE. Scale bar: 100 μm.

Previous studies have shown that $Ca^{2+}$ elevations induced by growth factors and neurotransmitters tightly regulate proliferation of NPCs. For example, EGF, a well-known regulator of NPC proliferation, mobilizes $Ca^{2+}$ signalling by activation of receptor-tyrosine-kinase coupled to the PLC–$InsP_3$ pathway (66); FGF2, another well-known regulator of NPC proliferation, induces $Ca^{2+}$ influx *via* TRPC1 channels (45). Likewise, glutamate, which triggers $Ca^{2+}$ mobilization, has long been reported to promote neural progenitor cell proliferation (67–70). In our study, increase in cellular $Ca^{2+}$ induced by 100 μM glutamate led to significant increase in cell proliferation, while reduction in intracellular $Ca^{2+}$ release with 50 μM 2-APB resulted in significant inhibition of cell proliferation in both ANPC genotypes. Furthermore, inhibition of upstream of $Ca^{2+}$ signalling by PLC inhibitor U73122 also significantly reduced cell proliferation. These findings indicated that appropriate higher intracellular $Ca^{2+}$ concentration leads to higher proliferation of ANPCs. Importantly, inhibition of intracellular $Ca^{2+}$ signalling abolished increased proliferation of HD ANPCs, strongly suggesting that enhanced $Ca^{2+}$ signalling contributed to the higher rate of proliferation in HD ANPCs.

Significant reduction in numbers of migrating cells from neurospheres has been found in the presence of T-type channel blockers (51), suggesting that entry of $Ca^{2+}$ from the extracellular medium plays a role in neural progenitor cell migration. Intracellular $Ca^{2+}$ stores have also been reported to affect migration of neural progenitor cells (NPC). One study from Pregno and colleagues showed that migratory activity induced by Neuregulin1 was through long-lasting increase in intracellular calcium concentration, dependent on release of $Ca^{2+}$ from internal stores (50). In our present study, inhibition of $Ca^{2+}$ release from internal stores with 2-APB or U73122, resulted in significantly reduced cell migration in both WT and YAC128 HD ANPCs,

indicating that $Ca^{2+}$ signalling was essential for active ANPC migration. Due to higher levels of $Ca^{2+}$ signalling in YAC128 HD ANPCs, YAC128 ANPCs moved significantly faster than WT controls.

In mouse embryonic stem cells, Neuronatin promoted neural induction through increasing intracellular $Ca^{2+}$ concentration, which in turn increased phosphorylation of Erk1/2, inhibited the BMP4 pathway and cooperated with the FGF/Erk pathway to induce neural generation (71). In cultured ANPCs isolated from rodent hippocampus, evoked intracellular $Ca^{2+}$ concentration was relayed to activation of transcription factor NeuroD, leading to neurogenesis (72). Similarly, isoxazole (a small molecule capable of triggering $Ca^{2+}$ influx via $Ca^{2+}$ channels and NMDA receptors), has been shown to induce robust neuronal differentiation in adult neural stem/progenitor cells (73). These findings indicate that increase in intracellular $Ca^{2+}$ is critical for neural fate determination. In our present study, due to higher levels of $Ca^{2+}$ signals in YAC128 HD ANPCs, YAC128 HD ANPCs differentiated into higher amounts of neurons with longer neurites than did WT controls, indicating that mutant HTT-induced elevated $Ca^{2+}$ signals actually enhanced potentials of HD ANPCs for neuronal differentiation and neuritogenesis.

Reactive oxygen species (ROS) overproduction has been implicated in pathogenesis of various neurodegenerative disorders such as Parkinson's (74), Alzheimer's (75) and Huntington's diseases (76). Besides their well-known toxicity, ROS can also play roles as second messengers, regulating various cellular functions including proliferation of NPCs/NSCs. Yoneyama *et al.* have observed that antioxidant treatments significantly inhibit hippocampal progenitor proliferation (60). Le Belle and colleagues reported that increases in endogenous ROS levels consistently enhanced neurosphere generation of neural stem cells (NSCs) derived from CNS, and addition of exogenous agents that elevate ROS levels increased production of neurospheres (61). In addition, endogenous production of ROS has been demonstrated to be necessary to maintain neural stem populations in the brain (77). In agreement with these findings, we found that YAC128 ANPCs manifested higher levels of endogenous ROS compared to WT cells. More importantly, HD ANPCs exhibited ROS signal-dependent enhancement of proliferation, as ROS scavenging abolished proliferation of both YAC128 and WT ANPCs. ROS might also be linked to cell migration. In haematopoietic stem cells, it has been shown that low level of ROS can retain stem cell quiescence, while high levels of ROS promote their migration (78). In our study, YAC128 ANPCs had higher ROS levels than WT cells; accordingly, they also showed ROS signal-dependent increases in cell migration capability.

Our experiments demonstrate that YAC128 HD ANPCs not only maintained their "stemness", but also had increased capabilities for proliferation, migration and neuronal differentiation *in vitro*. But *in vivo*, YAC128 mice brains failed to show any enhancement in ANPC proliferation/neuronal differentiation in the SVZ compared to WT mice, even by 18-months of age, a time point at which the YAC128 mice not only exhibited behavioural and neuropathological changes (including neuronal loss) but also presented huntingtin inclusions in striatal cells (31). These observations strongly suggest that the striatal micro-environment severely constrained neurogenesis in the SVZ, and failed to provide appropriate signals for generating new neurons to replace dead ones in YAC128 mouse brains. Given that the intrinsic potentials of HD ANPCs for proliferation and differentiation had not been impaired (were actually enhanced), endogenous cell repair strategies are potentially possible in HD, and may require exogenous factors to up-regulate ANPC proliferation and neurogenesis (72,79–83). However, our present study suggests that the SVZ micro-environment in which ANPCs are organized limits adult neurogenesis in HD mouse brains. Thus, remoulding the micro-environment into a suitable condition for endogenous neurogenesis, is critical for cell repair strategies.

Under neurodegenerative conditions in the SVZ of YAC128 mouse brains, intrinsic properties of HD ANPCs were not impaired. In contrast, mutant HTT-induced elevated $Ca^{2+}$ and ROS signalling conferred HD ANPCs with enhanced capabilities of proliferation, migration and neuronal differentiation. Additional pathways could also contribute to these phenotypes. A recent unbiased RNAi screen for modifiers of HD pathogenesis identified RRAS signalling as an affected pathway, which plays a role in both cell migration and neurite outgrowth (84). Interestingly, the *in vivo* micro-environment did not support endogenous ANPCs to respond appropriately to neuronal loss in YAC128 mouse brains. Thus, how to liberate ANPCs from their constrained micro-environment, by remoulding the niche, is a crucial step for cell replacement therapy in HD.

## Acknowledgements

We apologize to those investigators whose work we could not cite due to the space limit, and gratefully acknowledge their contributions to Huntington's disease field. We thank Zhongyang Qv and Yihan Wang for help with maintaining the YAC128 mouse colony, Ilya Bezprozvanny for facilitating transportation of mice

 

strains, Zhifeng Xiao and Baoyang Hu for help with neural progenitor cell culture, and Caixia Guo for helpful discussion. This work was supported by grants from the National Basic Research Program of China (2011CB965003, 2012CB944702), NSFC (81371415, 31401151, 81300982), and the CAS/SAFEA International Partnership Program for Creative Research Teams.

## Competing interests

The authors of the manuscript declare no conflict of interests.

## Reference

1 Alvarez-Buylla A, Lim DA (2004) For the long run: maintaining germinal niches in the adult brain. *Neuron* **41**, 683–686.
2 Zhao C, Deng W, Gage FH (2008) Mechanisms and functional implications of adult neurogenesis. *Cell* **132**, 645–660.
3 Gheusi G, Cremer H, McLean H, Chazal G, Vincent JD, Lledo PM (2000) Importance of newly generated neurons in the adult olfactory bulb for odor discrimination. *Proc. Natl Acad. Sci. USA* **97**, 1823–1828.
4 Carleton A, Petreanu LT, Lansford R, Alvarez-Buylla A, Lledo PM (2003) Becoming a new neuron in the adult olfactory bulb. *Nat. Neurosci.* **6**, 507–518.
5 Imayoshi I, Sakamoto M, Ohtsuka T, Takao K, Miyakawa T, Yamaguchi M *et al.* (2008) Roles of continuous neurogenesis in the structural and functional integrity of the adult forebrain. *Nat. Neurosci.* **11**, 1153–1161.
6 Shors TJ, Miesegaes G, Beylin A, Zhao M, Rydel T, Gould E (2001) Neurogenesis in the adult is involved in the formation of trace memories. *Nature* **410**, 372–376.
7 van Praag H, Schinder AF, Christie BR, Toni N, Palmer TD, Gage FH (2002) Functional neurogenesis in the adult hippocampus. *Nature* **415**, 1030–1034.
8 Kitamura T, Saitoh Y, Takashima N, Murayama A, Niibori Y, Ageta H *et al.* (2009) Adult neurogenesis modulates the hippocampus-dependent period of associative fear memory. *Cell* **139**, 814–827.
9 Arvidsson A, Collin T, Kirik D, Kokaia Z, Lindvall O (2002) Neuronal replacement from endogenous precursors in the adult brain after stroke. *Nat. Med.* **8**, 963–970.
10 Nakatomi H, Kuriu T, Okabe S, Yamamoto S, Hatano O, Kawahara N *et al.* (2002) Regeneration of hippocampal pyramidal neurons after ischemic brain injury by recruitment of endogenous neural progenitors. *Cell* **110**, 429–441.
11 Liu F, You Y, Li X, Ma T, Nie Y, Wei B *et al.* (2009) Brain injury does not alter the intrinsic differentiation potential of adult neuroblasts. *J. Neurosci.* **29**, 5075–5087.
12 Martino G, Pluchino S, Bonfanti L, Schwartz M (2011) Brain regeneration in physiology and pathology: the immune signature driving therapeutic plasticity of neural stem cells. *Physiol. Rev.* **91**, 1281–1304.
13 Pieper AA, Xie S, Capota E, Estill SJ, Zhong J, Long JM *et al.* (2010) Discovery of a proneurogenic, neuroprotective chemical. *Cell* **142**, 39–51.
14 Hsieh J, Eisch AJ (2010) Epigenetics, hippocampal neurogenesis, and neuropsychiatric disorders: unraveling the genome to understand the mind. *Neurobiol. Dis.* **39**, 73–84.
15 Jin K, Peel AL, Mao XO, Xie L, Cottrell BA, Henshall DC *et al.* (2004) Increased hippocampal neurogenesis in Alzheimer's disease. *Proc. Natl Acad. Sci. USA* **101**, 343–347.
16 Verret L, Jankowsky JL, Xu GM, Borchelt DR, Rampon C (2007) Alzheimer's-type amyloidosis in transgenic mice impairs survival of newborn neurons derived from adult hippocampal neurogenesis. *J. Neurosci.* **27**, 6771–6780.
17 Li B, Yamamori H, Tatebayashi Y, Shafit-Zagardo B, Tanimukai H, Chen S *et al.* (2008) Failure of neuronal maturation in Alzheimer disease dentate gyrus. *J. Neuropathol. Exp. Neurol.* **67**, 78–84.
18 Hoglinger GU, Rizk P, Muriel MP, Duyckaerts C, Oertel WH, Caille I *et al.* (2004) Dopamine depletion impairs precursor cell proliferation in Parkinson disease. *Nat. Neurosci.* **7**, 726–735.
19 Crews L, Mizuno H, Desplats P, Rockenstein E, Adame A, Patrick C *et al.* (2008) Alpha-synuclein alters Notch-1 expression and neurogenesis in mouse embryonic stem cells and in the hippocampus of transgenic mice. *J. Neurosci.* **28**, 4250–4260.
20 Winner B, Rockenstein E, Lie DC, Aigner R, Mante M, Bogdahn U *et al.* (2008) Mutant alpha-synuclein exacerbates age-related decrease of neurogenesis. *Neurobiol. Aging* **29**, 913–925.
21 Gil JM, Mohapel P, Araujo IM, Popovic N, Li JY, Brundin P *et al.* (2005) Reduced hippocampal neurogenesis in R6/2 transgenic Huntington's disease mice. *Neurobiol. Dis.* **20**, 744–751.
22 Lazic SE, Grote H, Armstrong RJ, Blakemore C, Hannan AJ, van Dellen A *et al.* (2004) Decreased hippocampal cell proliferation in R6/1 Huntington's mice. *NeuroReport* **15**, 811–813.
23 McCollum MH, Leon RT, Rush DB, Guthrie KM, Wei J (2013) Striatal oligodendrogliogenesis and neuroblast recruitment are increased in the R6/2 mouse model of Huntington's disease. *Brain Res.* **1518**, 91–103.
24 Simpson JM, Gil-Mohapel J, Pouladi MA, Ghilan M, Xie Y, Hayden MR *et al.* (2011) Altered adult hippocampal neurogenesis in the YAC128 transgenic mouse model of Huntington disease. *Neurobiol. Dis.* **41**, 249–260.
25 Li S, Li XJ (2006) Multiple pathways contribute to the pathogenesis of Huntington disease. *Mol. Neurodegener.* **1**, 19.
26 Gil JM, Rego AC (2008) Mechanisms of neurodegeneration in Huntington's disease. *Eur. J. Neurosci.* **27**, 2803–2820.
27 Rosas HD, Koroshetz WJ, Chen YI, Skeuse C, Vangel M, Cudkowicz ME *et al.* (2003) Evidence for more widespread cerebral pathology in early HD: an MRI-based morphometric analysis. *Neurology* **60**, 1615–1620.
28 Molero AE, Gokhan S, Gonzalez S, Feig JL, Alexandre LC, Mehler MF (2009) Impairment of developmental stem cell-mediated striatal neurogenesis and pluripotency genes in a knock-in model of Huntington's disease. *Proc. Natl Acad. Sci. USA* **106**, 21900–21905.
29 Ritch JJ, Valencia A, Alexander J, Sapp E, Gatune L, Sangrey GR *et al.* (2012) Multiple phenotypes in Huntington disease mouse neural stem cells. *Mol. Cell Neurosci.* **50**, 70–81.
30 Curtis MA, Penney EB, Pearson AG, van Roon-Mom WM, Butterworth NJ, Dragunow M *et al.* (2003) Increased cell proliferation and neurogenesis in the adult human Huntington's disease brain. *Proc. Natl Acad. Sci. USA* **100**, 9023–9027.
31 Slow EJ, van Raamsdonk J, Rogers D, Coleman SH, Graham RK, Deng Y *et al.* (2003) Selective striatal neuronal loss in a YAC128 mouse model of Huntington disease. *Hum. Mol. Genet.* **12**, 1555–1567.
32 Ehrnhoefer DE, Butland SL, Pouladi MA, Hayden MR (2009) Mouse models of Huntington disease: variations on a theme. *Dis. Model Mech.* **2**, 123–129.
33 Zeron MM, Hansson O, Chen N, Wellington CL, Leavitt BR, Brundin P *et al.* (2002) Increased sensitivity to N-methyl-D-aspartate

receptor-mediated excitotoxicity in a mouse model of Huntington's disease. *Neuron* **33**, 849–860.
34 Tang TS, Tu H, Chan EY, Maximov A, Wang Z, Wellington CL *et al.* (2003) Huntingtin and huntingtin-associated protein 1 influence neuronal calcium signaling mediated by inositol-(1,4,5)\ triphosphate receptor type 1. *Neuron* **39**, 227–239.
35 Tang TS, Slow E, Lupu V, Stavrovskaya IG, Sugimori M, Llinas R *et al.* (2005) Disturbed Ca2 + signaling and apoptosis of medium spiny neurons in Huntington's disease. *Proc. Natl Acad. Sci. USA* **102**, 2602–2607.
36 Fan MM, Fernandes HB, Zhang LY, Hayden MR, Raymond LA (2007) Altered NMDA receptor trafficking in a yeast artificial chromosome transgenic mouse model of Huntington's disease. *J. Neurosci.* **27**, 3768–3779.
37 Bezprozvanny I (2009) Calcium signaling and neurodegenerative diseases. *Trends Mol. Med.* **15**, 89–100.
38 Perez-Severiano F, Rios C, Segovia J (2000) Striatal oxidative damage parallels the expression of a neurological phenotype in mice transgenic for the mutation of Huntington's disease. *Brain Res.* **862**, 234–237.
39 Wang JQ, Chen Q, Wang X, Wang QC, Wang Y, Cheng HP *et al.* (2013) Dysregulation of mitochondrial calcium signaling and superoxide flashes cause mitochondrial genomic DNA damage in Huntington disease. *J. Biol. Chem.* **288**, 3070–3084.
40 Spiliotopoulos D, Goffredo D, Conti L, Di Febo F, Biella G, Toselli M *et al.* (2009) An optimized experimental strategy for efficient conversion of embryonic stem (ES)-derived mouse neural stem (NS) cells into a nearly homogeneous mature neuronal population. *Neurobiol. Dis.* **34**, 320–331.
41 Suh H, Consiglio A, Ray J, Sawai T, D'Amour KA, Gage FH (2007) In vivo fate analysis reveals the multipotent and self-renewal capacities of Sox2 + neural stem cells in the adult hippocampus. *Cell Stem Cell* **1**, 515–528.
42 Thier M, Worsdorfer P, Lakes YB, Gorris R, Herms S, Opitz T *et al.* (2012) Direct conversion of fibroblasts into stably expandable neural stem cells. *Cell Stem Cell* **10**, 473–479.
43 Gage FH (2000) Mammalian neural stem cells. *Science* **287**, 1433–1438.
44 Ryu JK, Choi HB, Hatori K, Heisel RL, Pelech SL, McLarnon JG *et al.* (2003) Adenosine triphosphate induces proliferation of human neural stem cells: role of calcium and p70 ribosomal protein S6 kinase. *J. Neurosci. Res.* **72**, 352–362.
45 Fiorio Pla A, Maric D, Brazer SC, Giacobini P, Liu X, Chang YH *et al.* (2005) Canonical transient receptor potential 1 plays a role in basic fibroblast growth factor (bFGF)/FGF receptor-1-induced Ca2 + entry and embryonic rat neural stem cell proliferation. *J. Neurosci.* **25**, 2687–2701.
46 Gilley JA, Kernie SG (2011) Excitatory amino acid transporter 2 and excitatory amino acid transporter 1 negatively regulate calcium-dependent proliferation of hippocampal neural progenitor cells and are persistently upregulated after injury. *Eur. J. Neurosci.* **34**, 1712–1723.
47 Somasundaram A, Shum AK, McBride HJ, Kessler JA, Feske S, Miller RJ *et al.* (2014) Store-operated CRAC channels regulate gene expression and proliferation in neural progenitor cells. *J. Neurosci.* **34**, 9107–9123.
48 Scemes E, Duval N, Meda P (2003) Reduced expression of P2Y1 receptors in connexin43-null mice alters calcium signaling and migration of neural progenitor cells. *J. Neurosci.* **23**, 11444–11452.
49 McKinney MC, Kulesa PM (2011) In vivo calcium dynamics during neural crest cell migration and patterning using GCaMP3. *Dev. Biol.* **358**, 309–317.
50 Pregno G, Zamburlin P, Gambarotta G, Farcito S, Licheri V, Fregnan F *et al.* (2011) Neuregulin1/ErbB4-induced migration in ST14A striatal progenitors: calcium-dependent mechanisms and modulation by NMDA receptor activation. *BMC Neurosci.* **12**, 103.
51 Louhivuori LM, Louhivuori V, Wigren HK, Hakala E, Jansson LC, Nordstrom T *et al.* (2013) Role of low voltage activated calcium channels in neuritogenesis and active migration of embryonic neural progenitor cells. *Stem Cells Dev.* **22**, 1206–1219.
52 Estrada M, Cardenas C, Liberona JL, Carrasco MA, Mignery GA, Allen PD *et al.* (2001) Calcium transients in 1B5 myotubes lacking ryanodine receptors are related to inositol trisphosphate receptors. *J. Biol. Chem.* **276**, 22868–22874.
53 Gulbransen BD, Bashashati M, Hirota SA, Gui X, Roberts JA, MacDonald JA *et al.* (2012) Activation of neuronal P2X7 receptor-pannexin-1 mediates death of enteric neurons during colitis. *Nat. Med.* **18**, 600–604.
54 Zheng JQ, Poo MM (2007) Calcium signaling in neuronal motility. *Annu. Rev. Cell Dev. Biol.* **23**, 375–404.
55 Charvin D, Vanhoutte P, Pages C, Borrelli E, Caboche J (2005) Unraveling a role for dopamine in Huntington's disease: the dual role of reactive oxygen species and D2 receptor stimulation. *Proc. Natl Acad. Sci. USA* **102**, 12218–12223.
56 Li X, Valencia A, Sapp E, Masso N, Alexander J, Reeves P *et al.* (2010) Aberrant Rab11-dependent trafficking of the neuronal glutamate transporter EAAC1 causes oxidative stress and cell death in Huntington's disease. *J. Neurosci.* **30**, 4552–4561.
57 Dong G, Ferguson JM, Duling AJ, Nicholas RG, Zhang D, Rezvani K *et al.* (2011) Modeling pathogenesis of Huntington's disease with inducible neuroprogenitor cells. *Cell. Mol. Neurobiol.* **31**, 737–747.
58 Finkel T, Holbrook NJ (2000) Oxidants, oxidative stress and the biology of ageing. *Nature* **408**, 239–247.
59 Studer L, Csete M, Lee SH, Kabbani N, Walikonis J, Wold B *et al.* (2000) Enhanced proliferation, survival, and dopaminergic differentiation of CNS precursors in lowered oxygen. *J. Neurosci.* **20**, 7377–7383.
60 Yoneyama M, Kawada K, Gotoh Y, Shiba T, Ogita K (2010) Endogenous reactive oxygen species are essential for proliferation of neural stem/progenitor cells. *Neurochem. Int.* **56**, 740–746.
61 Le Belle JE, Orozco NM, Paucar AA, Saxe JP, Mottahedeh J, Pyle AD *et al.* (2011) Proliferative neural stem cells have high endogenous ROS levels that regulate self-renewal and neurogenesis in a PI3K/Akt-dependant manner. *Cell Stem Cell* **8**, 59–71.
62 Noble M, Proschel C, Mayer-Proschel M (2011) Oxidative-reductionist approaches to stem and progenitor cell function. *Cell Stem Cell* **8**, 1–2.
63 Hurd TR, DeGennaro M, Lehmann R (2012) Redox regulation of cell migration and adhesion. *Trends Cell Biol.* **22**, 107–115.
64 Shi D, Li X, Chen H, Che N, Zhou S, Lu Z *et al.* (2014) High level of reactive oxygen species impaired mesenchymal stem cell migration via overpolymerization of F-actin cytoskeleton in systemic lupus erythematosus. *Pathol. Biol. (Paris)* **62**, 382–390.
65 Yang CM, Hsieh HL, Yu PH, Lin CC, Liu SW (2015) IL-1beta Induces MMP-9-Dependent Brain Astrocytic Migration via Transactivation of PDGF Receptor/NADPH Oxidase 2-Derived Reactive Oxygen Species Signals. *Mol. Neurobiol.* **52**, 303–317.
66 Maric D, Maric I, Chang YH, Barker JL (2003) Prospective cell sorting of embryonic rat neural stem cells and neuronal and glial progenitors reveals selective effects of basic fibroblast growth factor and epidermal growth factor on self-renewal and differentiation. *J. Neurosci.* **23**, 240–251.

 

67 Brazel CY, Nunez JL, Yang Z, Levison SW (2005) Glutamate enhances survival and proliferation of neural progenitors derived from the subventricular zone. *Neuroscience* **131**, 55–65.
68 Di Giorgi-Gerevini V, Melchiorri D, Battaglia G, Ricci-Vitiani L, Ciceroni C, Busceti CL *et al.* (2005) Endogenous activation of metabotropic glutamate receptors supports the proliferation and survival of neural progenitor cells. *Cell Death Differ.* **12**, 1124–1133.
69 Suzuki M, Nelson AD, Eickstaedt JB, Wallace K, Wright LS, Svendsen CN (2006) Glutamate enhances proliferation and neurogenesis in human neural progenitor cell cultures derived from the fetal cortex. *Eur. J. Neurosci.* **24**, 645–653.
70 Nochi R, Kato T, Kaneko J, Itou Y, Kuribayashi H, Fukuda S *et al.* (2012) Involvement of metabotropic glutamate receptor 5 signaling in activity-related proliferation of adult hippocampal neural stem cells. *Eur. J. Neurosci.* **36**, 2273–2283.
71 Lin HH, Bell E, Uwanogho D, Perfect LW, Noristani H, Bates TJ *et al.* (2010) Neuronatin promotes neural lineage in ESCs via Ca (2 + ) signaling. *Stem Cells* **28**, 1950–1960.
72 Deisseroth K, Singla S, Toda H, Monje M, Palmer TD, Malenka RC (2004) Excitation-neurogenesis coupling in adult neural stem/progenitor cells. *Neuron* **42**, 535–552.
73 Schneider JW, Gao Z, Li S, Farooqi M, Tang TS, Bezprozvanny I *et al.* (2008) Small-molecule activation of neuronal cell fate. *Nat. Chem. Biol.* **4**, 408–410.
74 Przedborski S, Jackson-Lewis V, Vila M, Wu DC, Teismann P, Tieu K *et al.* (2003) Free radical and nitric oxide toxicity in Parkinson's disease. *Adv. Neurol.* **91**, 83–94.
75 Zhu X, Raina AK, Lee HG, Casadesus G, Smith MA, Perry G (2004) Oxidative stress signalling in Alzheimer's disease. *Brain Res.* **1000**, 32–39.
76 Lin MT, Beal MF (2006) Mitochondrial dysfunction and oxidative stress in neurodegenerative diseases. *Nature* **443**, 787–795.
77 Dickinson BC, Peltier J, Stone D, Schaffer DV, Chang CJ (2011) Nox2 redox signaling maintains essential cell populations in the brain. *Nat. Chem. Biol.* **7**, 106–112.
78 Ludin A, Gur-Cohen S, Golan K, Kaufmann KB, Itkin T, Medaglia C *et al.* (2014) Reactive oxygen species regulate hematopoietic stem cell self-renewal, migration and development, as well as their bone marrow microenvironment. *Antioxid. Redox Signal.* **21**, 1605–1619.
79 Jin K, LaFevre-Bernt M, Sun Y, Chen S, Gafni J, Crippen D *et al.* (2005) FGF-2 promotes neurogenesis and neuroprotection and prolongs survival in a transgenic mouse model of Huntington's disease. *Proc. Natl Acad. Sci. USA* **102**, 18189–18194.
80 Cho SR, Benraiss A, Chmielnicki E, Samdani A, Economides A, Goldman SA (2007) Induction of neostriatal neurogenesis slows disease progression in a transgenic murine model of Huntington disease. *J. Clin. Invest.* **117**, 2889–2902.
81 Duan W, Peng Q, Masuda N, Ford E, Tryggestad E, Ladenheim B *et al.* (2008) Sertraline slows disease progression and increases neurogenesis in N171-82Q mouse model of Huntington's disease. *Neurobiol. Dis.* **30**, 312–322.
82 Peng Q, Masuda N, Jiang M, Li Q, Zhao M, Ross CA *et al.* (2008) The antidepressant sertraline improves the phenotype, promotes neurogenesis and increases BDNF levels in the R6/2 Huntington's disease mouse model. *Exp. Neurol.* **210**, 154–163.
83 Decressac M, Wright B, Tyers P, Gaillard A, Barker RA (2010) Neuropeptide Y modifies the disease course in the R6/2 transgenic model of Huntington's disease. *Exp. Neurol.* **226**, 24–32.
84 Miller JP, Yates BE, Al-Ramahi I, Berman AE, Sanhueza M, Kim E *et al.* (2012) A genome-scale RNA-interference screen identifies RRAS signaling as a pathologic feature of Huntington's disease. *PLoS Genet.* **8**, e1003042.

## Supporting Information

Additional Supporting Information may be found in the online version of this article:

**Fig. S1** Effect of 2-APB (50 μM), U73122 (2 μM) and NAC (1 mM) on the apoptosis and necrosis of WT and YAC128 ANPCs. (a) Flow cytometry results after staining cells with Annexin V and PI. Cells were classified as healthy (Annexin $V^-$,$PI^-$), apoptotic (Annexin $V^+$, $PI^-$) and necrotic (Annexin $V^+$, $PI^+$). (b) Statistic analysis of the percentage of Annexin V-positive cells ($n = 3$). All of these drugs did not cause much cell death, and there were no significant differences between the genotypes in the percentage of Annexin $V^+$ cells.